ELSEVIER

Efficient drug discovery by rational lead hybridization based on crystallographic overlay

Shuo Zhang[1], Jian Zhang[1], Ping Gao[1], Lin Sun[1], Yuning Song[2], Dongwei Kang[1], Xinyong Liu[1] and Peng Zhan[1]

[1] Department of Medicinal Chemistry, Key Laboratory of Chemical Biology (Ministry of Education), School of Pharmaceutical Sciences, Shandong University, 44 West Culture Road, 250012, Ji'nan, Shandong, PR China
[2] Department of Clinical Pharmacy, Qilu Hospital of Shandong University, 250012, Ji'nan, Shandong, PR China

In this review, we provide an overview of recent applications of crystallographic overlay-based molecular structure hybridization of lead compounds as a rational strategy for efficient drug discovery, with selected examples, and briefly discuss its advantages compared with other ligand-based methodologies.

Introduction

Among medicinal chemistry strategies available for scaffold evolution in drug design and optimization, molecular hybridization is a robust approach. It aims to combine basic pharmacophore elements from diverse chemical entities with the same biological function (or two or more structural moieties with different bioactivities) to obtain a new hybrid entity with higher affinity and potency (or dual activities) [1,2]. Because the determination of high-resolution crystallographic structures of protein–inhibitor complexes has become increasingly routine, the amount of structural information available for inhibitor design has grown correspondingly. Such structural information reveals the interaction mode of an inhibitor, indicating key interactions that determine the binding affinity, and thus can reveal opportunities for evolving the scaffold and improving drug efficacy. Consequently, molecular hybridization based on crystallographic overlays (namely, knowledge-based pharmacophore hybridization) is an attractive design strategy to generate novel inhibitors from the structures of known ligands that bind to a common target. The method used the known positions of two or more ligands in the binding site to recombine fragments from each to generate a novel ligand, which will generally be a hybrid of the two scaffolds or a molecule generated by transfer of one or more substituents from one scaffold to the other. The latter approach is based on the idea that a potency-enhancing group from one scaffold should have a similar effect in a new scaffold, if positioned correctly [3]. Our goal in this review is to provide a broad overview of current applications of crystallographic overlay-based molecular hybridization for structure-based drug design, illustrated by selected recent examples.

Corresponding authors: Kang, D. (kangdongwei@sdu.edu.cn), Liu, X. (xinyongl@sdu.edu.cn), Zhan, P. (zhanpeng1982@sdu.edu.cn)

Case studies of crystallographic overlay-based molecular hybridization

HIV-1 non-nucleoside reverse transcriptase inhibitors

Owing to the development of drug resistance, there is an ongoing need for next-generation non-nucleoside reverse transcriptase (RT) inhibitors (NNRTIs) with different resistance profiles, improved safety, excellent tolerability and favorable physicochemical properties as antivirals to treat HIV infection [4–6]. In 2009, a crystallographic overlay-based molecular hybridization approach was used to create a new series of functionalized indazole derivatives that exhibit potent inhibition of wild-type (WT) and clinically relevant mutations of RT by combining pharmacophoric subunits of two reported NNRTIs: capravirine (**1**) and efavirenz (**2**) (Fig. 1a). Among the resulting compounds, **3a** and **3b** show potent antiviral activity and excellent metabolic stability [7]. On the basis of the reported co-crystal structure (Fig. 1b), **3a** binds to the allosteric binding site of RT with a highly similar conformation, compared to those of the precursor compounds. Remarkably, the indazole N–H shows H-bond interaction with the peptide main

https://doi.org/10.1016/j.drudis.2018.11.021

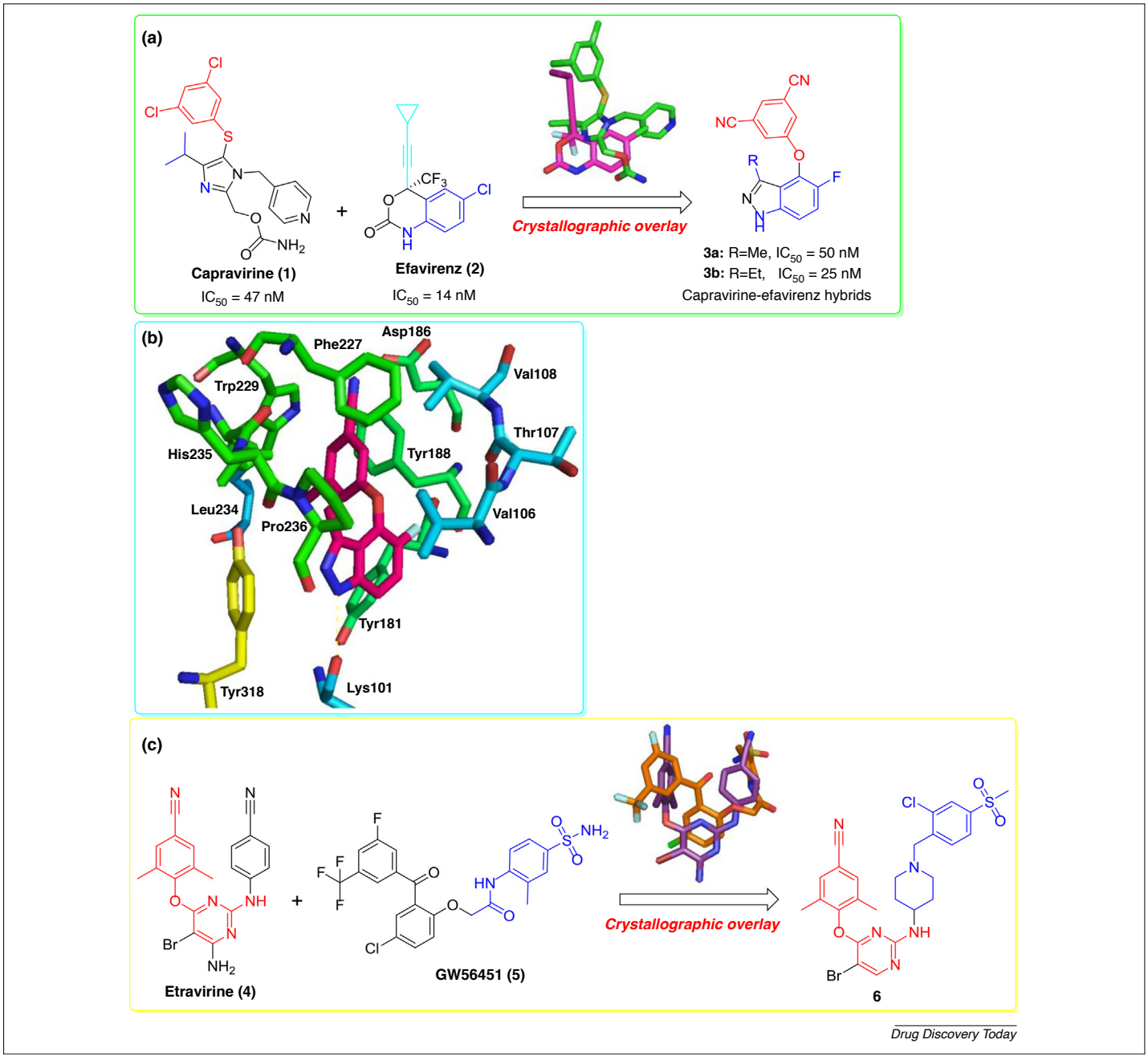

FIGURE 1

Design concept of functionalized indazole and piperidine-linked aminopyrimidine derivatives as potent NNRTIs. **(a)** Superposition of the X-ray crystal structures of capravirine (**1**, green) bound to wild-type HIV-1 RT (PDB code: 1EP4) and efavirenz (**2**, pink) bound to K103N RT (PDB code: 1FKO). **(b)** Cocrystal structure of **3a** with K103N mutant RT (pink, PDB code: 2JLE). Amino acid residues around the binding site were highlighted. **(c)** Overlay of crystal structures of etravirine (**4**, purple; PDB code: 3M8P) and GW564511 (**5**, deep yellow; PDB code: 3DLG) bound to HIV-1 RT.

chain of residue K101; and the cyano-substituted benzene ring displays edge-to-face π-interactions with the reserved W229 and a face-to-face π-interaction with the Y188 residue.

Several research groups, including ours, have spent many years focusing on the discovery of NNRTIs by applying knowledge-based pharmacophore hybridization [8–12]. For example, an analysis of the binding motifs of known HIV-1 NNRTIs etravirine (**4**) and GW564511 (**5**) afforded novel piperidine-linked aminopyrimidine derivatives with broad potency against WT and resistant variants (Fig. 1c). Notably, the series exhibits potency against the K103N, Y181C and Y188L variants, among others, as exemplified by the *N*-benzyl compound **6**, which has a particularly attractive profile [12].

HIV-1 protease inhibitors

Inspired by the HIV-1 protease-binding modes of MK-8718 (**7**) and PL-100 (**8**), a novel hybrid compound **9** was rationally designed and synthesized, as illustrated in Fig. 2. Further optimization resulted in HIV-1 protease inhibitor **10** bearing a bicyclic piperazine sulfonamide core; this compound showed a 60-fold improve-

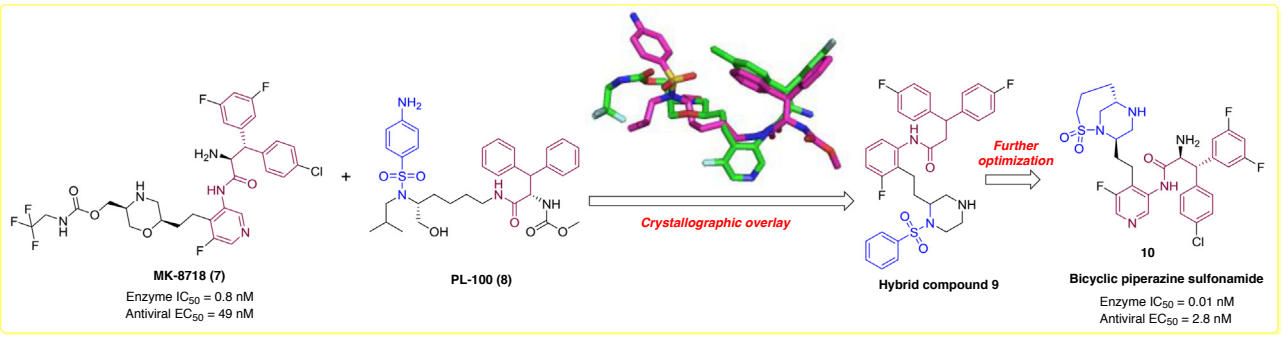

FIGURE 2

Development of piperazine sulfonamide-based HIV-1 protease inhibitors by means of crystallographic overlay-based molecular hybridization of MK-8718 (**7**, green; PDB code: 5IVT) and PL-100 (**8**, pink; PDB code: 2QMP).

ment in enzyme-binding affinity and a tenfold improvement in antiviral potency relative to **7** [13].

Phosphodiesterase type 4 inhibitors

Structure-guided molecular hybridization of oral phosphodiesterase type 4 (PDE4) inhibitor **11** by introducing fragments from **12** and clinical candidate GSK256066 (**13**) yielded dichloropyridyl-urea-pyridazinone **14** and naphthyridin-5(6H)-one **15**, respectively, which showed potent inhibition at picomolar levels (Fig. 3). The *meta* position of the pyridazinone 6-phenyl ring is oriented toward the solvent-filled pocket. Next, substituents with various physicochemical properties were introduced in the region occupying the solvent-filled pocket of PDE4, affording **16** and **17** as potent, long-acting and potentially safe inhaled PDE4 inhibitors. Compound **18** harboring a 1,6-naphthyridin-5(6H)-one *N*-oxide ring was the most active derivative of **15**, with an IC_{50} of 45 pM in an enzymatic assay and 75 pM in a cell-based assay [14,15].

Inhibitors of tyrosine kinase discoidin domain receptors DDR1 and DDR2

Tyrosine kinase discoidin domain receptors DDR1 and DDR2 have been implicated in several human diseases, including cancer. Based on the superimposition of the DDR1–fragment-**19** co-complex (PDB code: 5BVK) and the DDR1–dasatinib (**20**) co-complex (PDB code: 5BVW), fragment-based discovery and further optimization resulted in a low nanomolar-active, orally available inhibitor **21** which was selective for DDR1 and DDR2 over c-Src, in contrast to dasatinib. Compound **4** also showed promising *in vitro* PK and *in vivo* PK in mice (Fig. 4) [16].

Tankyrase inhibitors

Tankyrase (TNKS) is a poly-ADP-ribosylating protein (PARP), the activity of which suppresses cellular axin protein level and elevates β-catenin concentration, leading to increased oncogene expression. The inhibition of TNKS1 and TNKS2 has been shown to antagonize Wnt signaling via axin stabilization in APC mutant colon cancer cell lines [17]. In the following three instances, by using crystallographic overlays of the known TNKSI–TNKS complex as a starting point together with structure-based molecular hybridization, a novel class of potent and selective TNKSs with favorable pharmacokinetic properties was created.

Compound **22** was a previously disclosed TNKSI with moderate inhibitory activity (TNKS1, IC_{50} = 0.20 μM) that suffered from poor pharmacokinetic properties (the amide is prone to hydrolysis in rat and mouse plasma). The crucial interactions are three H-bonds: the C=O of the amide with D1198; the C=O of the oxazolidinone with Y1213; and a C=O···H–C-type H-bond between the hydrogen at C-6 of the quinoline and the backbone C=O of G1196 (TNKS1). In addition, the quinoline ring is involved in a π-stacking interaction with H1201. Overlay of the TNKS–TNKSI co-crystal structures of HTS hit **23** (TNKS1 IC_{50} = 0.024 μM) and **20** (Fig. 5) exhibited that the C=O group of the benzimidazolone and the amide moiety are engaged in H-bond interactions with D1198. In addition, the electron-deficient quinoline moiety of **22** overlaid well with the benzimidazolone phenyl moiety of **23**; and was associated with a close stacking interaction with H1201. Based on the above analysis, the combination of the oxazolidinone group of **22** with the cyclohexyl benzimidazolone of **23** generated **24** and **25** (after further modification), which showed enhanced potency (TNKS1 IC_{50} = 4 nM and 1 nM, respectively) and good pharmacokinetic properties, including favorable oral bioavailability [18].

Compound **26** was discovered as a novel and potent TNKSI via a HTS approach (TNKS IC_{50} = 0.15 μM; TBC IC_{50} = 2.0 μM; PARP1 IC_{50} > 85 μM). A co-crystal structure of the TNKS1–**26** complex suggested that **26** simultaneously occupied the conserved nicotinamide pocket and the induced pocket. The dihydroquinolinone moiety resided in the nicotinamide pocket with the C=O group engaging in a H-bond interaction with S1221, and the nitrogen formed a H-bond to G1185. The aminoquinazoline group occupied the induced pocket, with the amino moiety H-bonding with G1196, and N1 H-bonding with D1198 (Fig. 5) [19]. An overlay of the co-crystal structures of **22** and **26** in the complex with TNKS1 suggested that replacing the labile aminoquinazoline amide of **26** with other counterparts would mitigate metabolic liabilities in plasma while retaining the two key H-bond interactions with the target (Fig. 5).

It was envisioned that the aminopyridine group would serve as a simplified mimic of the aminoquinazoline ring in **26**. Placing a pyrimidinyl moiety in the 3-position would enable the crucial π-stacking interaction with H1201, as observed with the quinoline

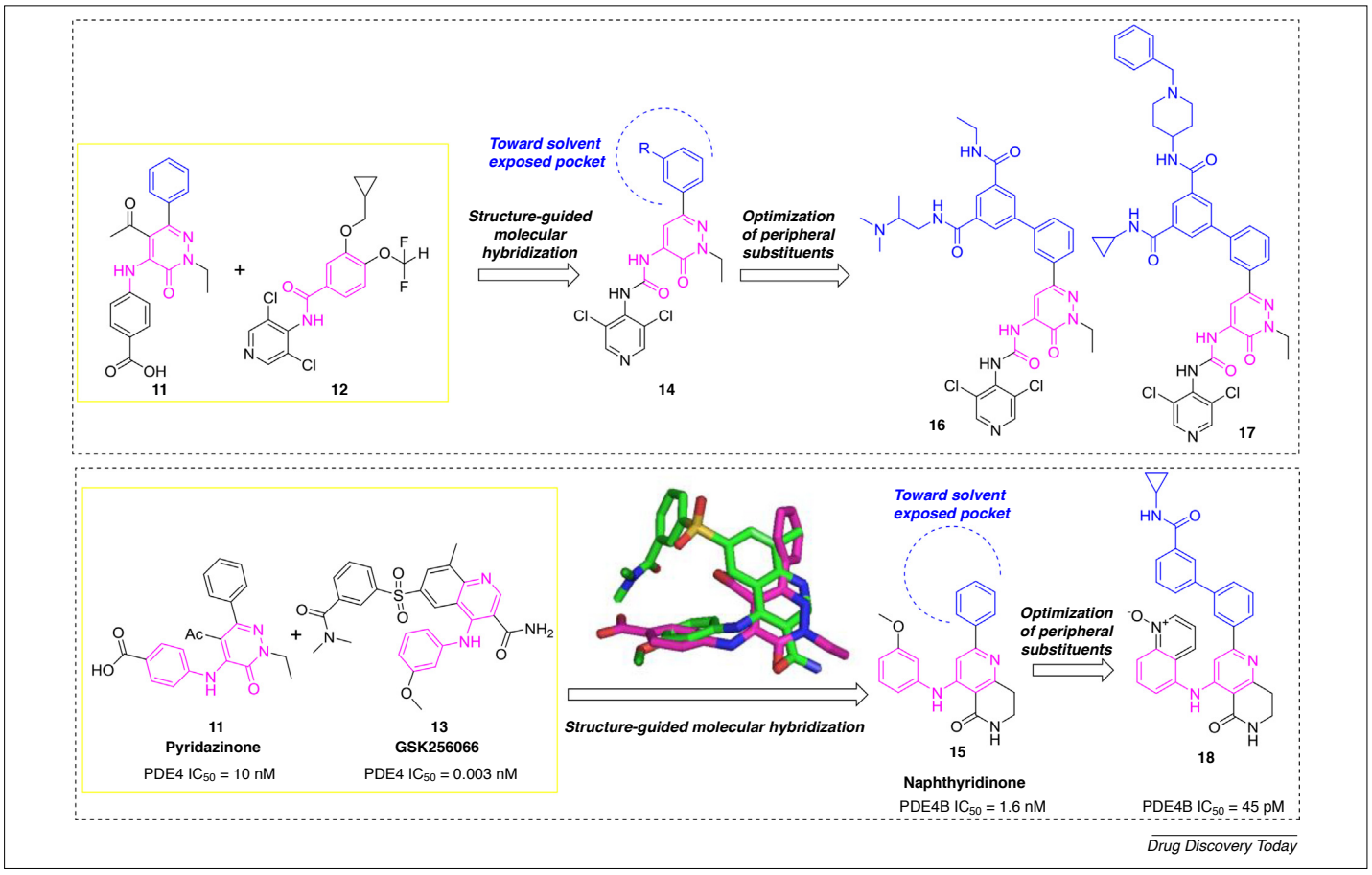

FIGURE 3

Novel PDE4 inhibitors designed by means of molecular hybridization based on crystallographic overlays, and further optimization of peripheral substituents for the solvent-exposed region. The X-ray structures of **11** (pink; PDB code: 5K1I) and roflumilast **12** (blue; PDB code: 1XOQ), and GSK256066 (**13**, green; PDB code: 3GWT), were utilized.

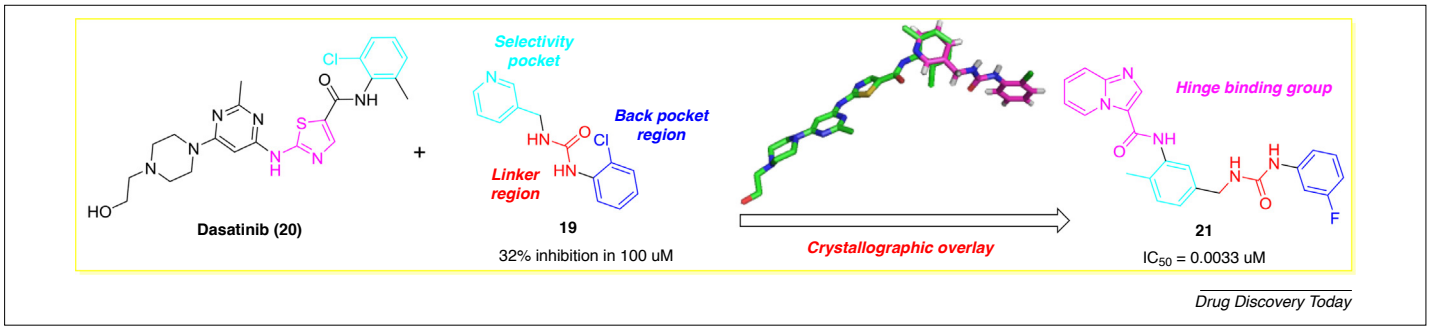

FIGURE 4

Schematic of the design process based on the superimposition of the DDR1–fragment-**19** co-complex (PDB code: 5BVK) and the DDR1–dasatinib (**20**) co-complex (PDB code: 5BVW).

group in **22**. Indeed, it was gratifying that **27** exhibited high TNKS-inhibitory potency while showing favorable selectivity vs PARP1/2. Compound **27** promoted accumulation of axin (EC_{50} = 0.709 μM) and suppressed β-catenin accumulation (TBC IC_{50} = 0.233 μM) and Wnt reporter gene transcription (STF IC_{50} = 0.096 μM) in cellular assays. Furthermore, it was stable in the presence of rat and human liver microsomes (RLM/HLM Clint = 48/33 μl/min/mg) [19].

In a similar way, a structure-guided hybridization approach was used to join the privileged diaryl-substituted 1,2,4-triazole and the benzimidazolone moiety from the two inhibitors **29** and **23**, in which the available co-crystal structures of TNKS2–**29** and TNKS1–**23** analogs were used to guide the hybrid and linker design. This approach gave immediate access to a new class of TNKSIs, as exemplified by **30**, which displays high affinity for TNKS1/2, with biochemical IC_{50} values of 29 nM and 6.3 nM,

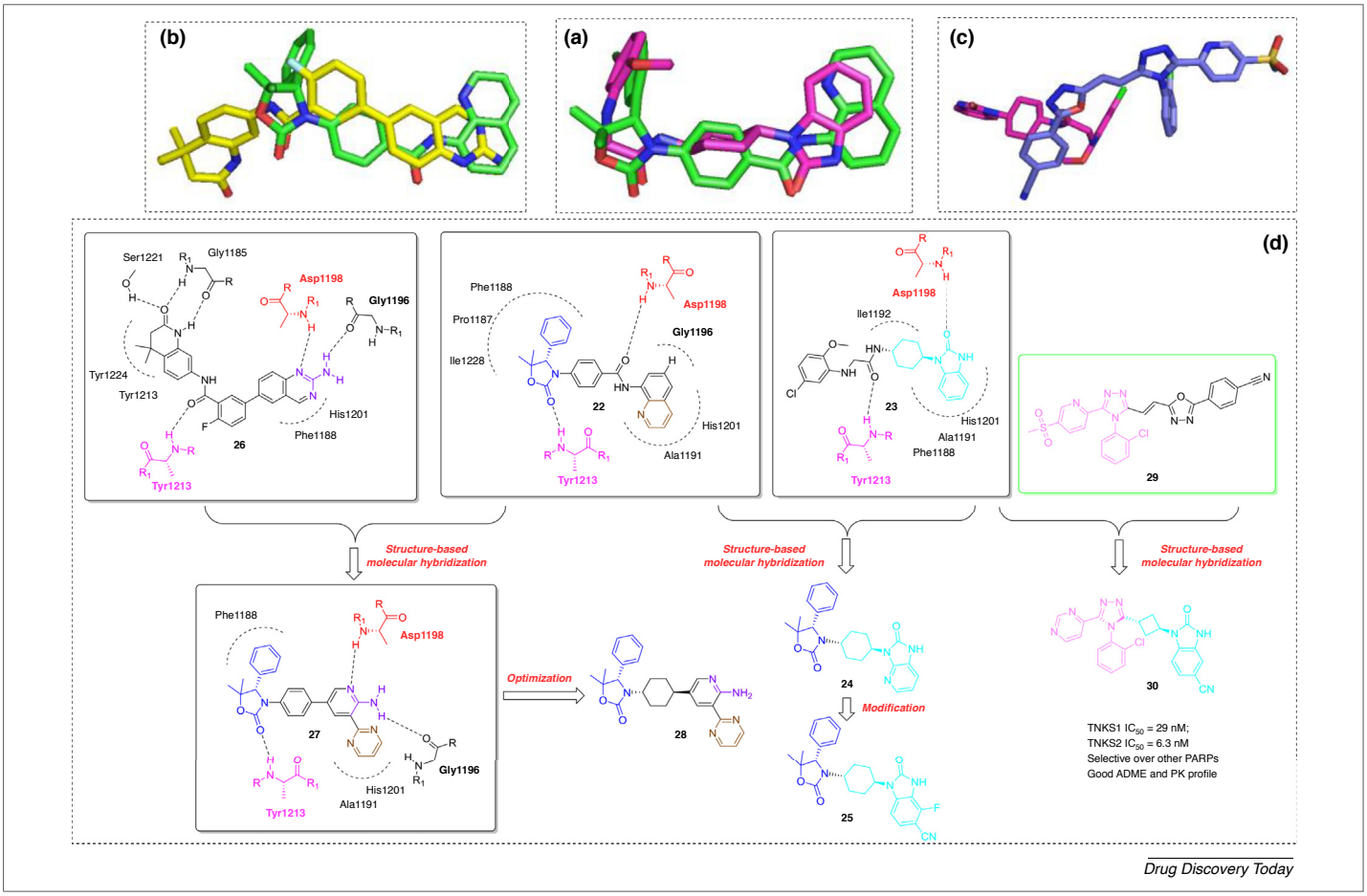

FIGURE 5

(a) Overlay of the TNKS1 co-crystal structure of **22** (red; PDB code: 4K4F) and **23** (green; PDB code: 4K4E) [18]. **(b)** Overlay of the TNKS1 co-crystal structure of **22** (red; PDB code: 4K4F) and **26** (blue; PDB code: 4N3R) [19]. **(c)** Overlay of the TNKS2 co-crystal structure of **29** (red; PDB: 4HYF) and the TNKS2 co-crystal structure of **23** (green; PDB code: 4K4E) [20]. **(d)** Chemdraw representation of crystallographic overlay-based molecular hybridization.

respectively, and a cellular IC_{50} value of 19 nM; it also shows high selectivity for TNKS over other poly(ADP-ribose) polymerases (Fig. 5). The identified inhibitor has a favorable *in vitro* ADME profile and shows good oral bioavailability in mice, rats and dogs [20].

Leishmania N-*myristoyltransferase inhibitors*

Leishmania N-myristoyltransferase (NMT) has been validated chemically and biologically as a potential target for the treatment of leishmaniasis. Comparison of the distinct binding modes of hits **31** and **32** demonstrated that the benzo-ring of the indole in **31** and the aromatic substituent of the pyrrolidine in **32** bind in the same region (Fig. 6). For this reason, it was hypothesized that addition of a *para*-fluorophenyl acetamide group *ortho* to the chlorine atom in this ring in **32** would substantially improve the activity by enabling H-bond formation between the acetamide carbonyl and Y345 and N376 and allowing **32** to extend into the same hydrophobic pocket as **31**. Based on these structural insights, the enzyme-inhibitory activity was increased 40-fold via hybridization of the two distinct binding modes, affording a novel, highly active and selective (over the human enzyme) *Leishmania donovani* NMT inhibitor **33** [21].

Reversible factor D inhibitors

The highly specific S1 serine protease factor D (FD) plays an important part in amplification of the complement alternative pathway (AP) of the innate immune system. The crystal structure of the complex between human FD and **34** (pink; PDB code 5NAT) overlaid with FD-bound **35** (cyan; PDB code 5FBI) revealed multiple H-bond interactions: urea carbonyl of **34** to G193 NH (oxyanion hole), amide NH of **34** to the backbone carbonyl of L41, terminal carboxamide of **35** to T214 of the self-inhibitory loop and to R218 at the bottom of the S1 pocket and indole-NH of **35** to the R218 main-chain carbonyl. Further, the benzoic acid portion of **35** is positioned in the solvent space and is not resolved in the crystal structure. Based on these findings, structure-based optimization of the (*S*)-proline-based lead **34** afforded the noncovalent, reversible, selective and orally bioavailable human FD inhibitor **36** with drug-like properties. This compound displayed outstanding potency in 50% human whole-blood *in vitro* and inhibited AP activity *ex vivo* after oral administration to monkeys. It showed excellent oral and ocular efficacy in a lipopolysaccharide (LPS)-induced mouse model (Fig. 7) [22].

Autotaxin inhibitors

Autotaxin (ATX) generates the bioactive lipid lysophosphatidic acid (LPA) and is a drug target of interest for numerous patholo-

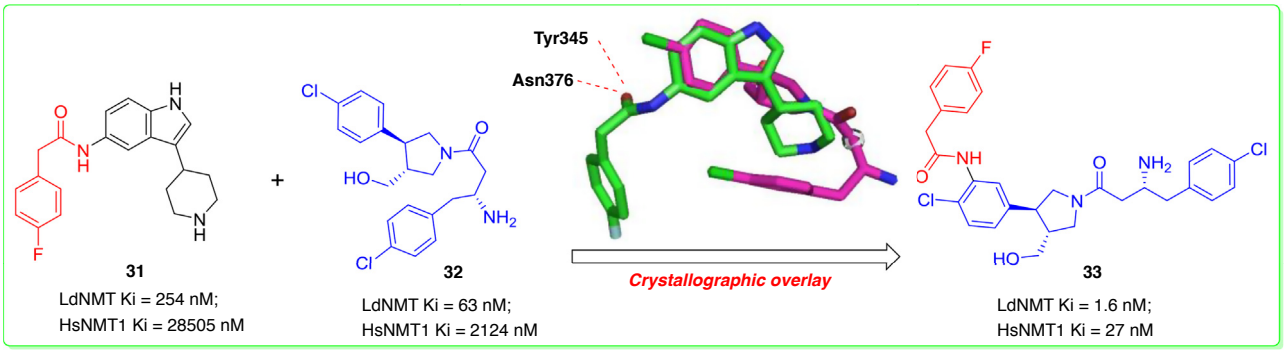

FIGURE 6

Discovery of potent and selective *Leishmania N*-myristoyltransferase inhibitors via hybridization based on the binding modes of compound **31** (green; PDB code: 4CGN) and compound **32** (pink; PDB code: 4CGL) in the peptide-binding pocket of *Leishmania* NMT. Note: *Leishmania donovani* (Ld); there are two human isoforms of NMT (HsNMT1 and HsNMT2).

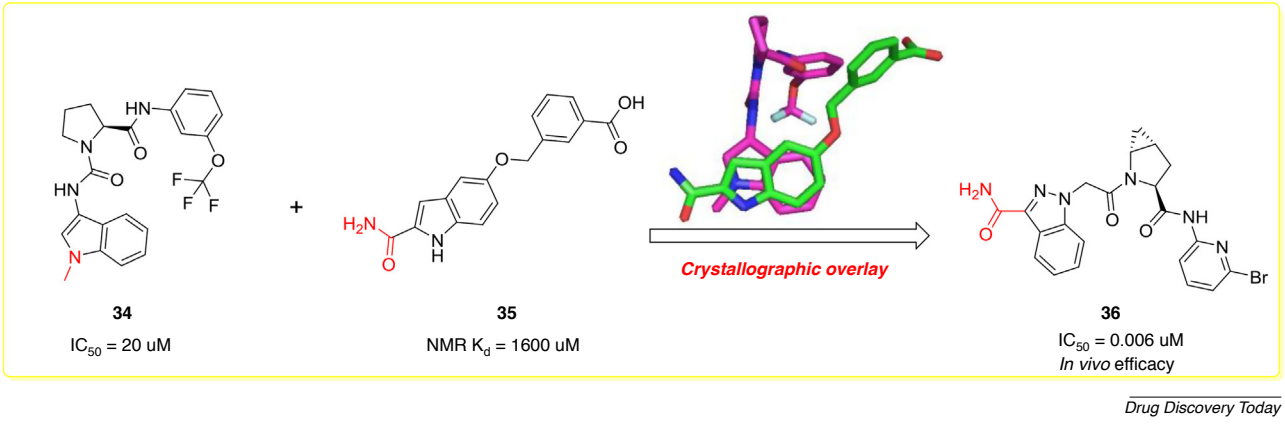

FIGURE 7

(a) Crystal structure of the complex between human FD and **34** (pink; PDB code: 5NAT) overlaid with FD-bound **35** (green; PDB code: 5FBI). **(b)** Design concept of reversible factor D inhibitors.

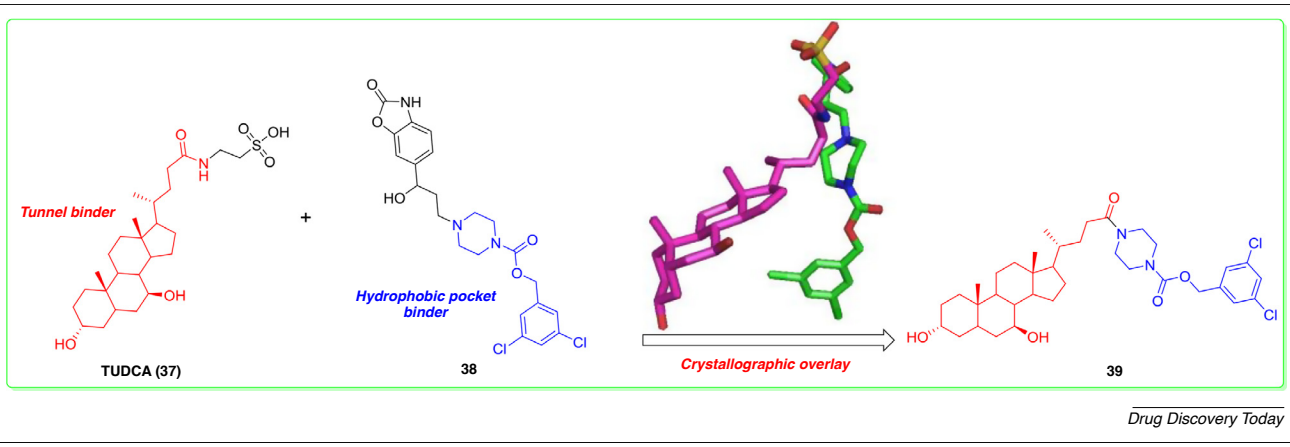

FIGURE 8

Hybrid design concept based on the binding modes of **37** (cyan; PDB code: 5DLW) and **38** (green; PDB code: 5M0E) to autotaxin. **37** and **38** bind to the tunnel and the hydrophobic pocket of autotaxin, respectively.

gies. ATX has a tripartite active site, including a hydrophilic groove, a hydrophobic lipid-binding pocket and a tunnel of unclear function. Weak physiological allosteric inhibitors **37** and **38** bind to the hydrophobic pocket and the tunnel of ATX, respectively. Based on the hybrid design concept, structure-guided evolution of these compounds afforded a potent competitive ATX inhibitor **39** that does not interact with the catalytic site. This compound attenuated LPA-mediated signaling in cells and reduced LPA synthesis *in vivo* and is expected to be a valuable tool for exploring the pathophysiological roles of ATX (Fig. 8) [23].

Lysine-specific demethylase 1 inhibitors

Because lysine-specific demethylase 1 (LSD1) regulates the maintenance of cancer stem cell properties, small-molecular inhibitors of LSD1 are expected to be useful for the treatment of several cancers [24]. By combining information from crystallographic overlays of the FAD–PCPA (**40**) conjugate and the reduced FAD-*N*-propargyl lysine peptide conjugate bound to the catalytic site of LSD1, a novel series of small-molecular LSD1-selective inhibitors was developed (Fig. 9). As expected, compounds **41** and NCL1 (**42**) inhibited H3K4 methylation *in vivo*. Notably, **42** is the first LSD1-selective inhibitor in cellular assays, and it was able to effectively inhibit prostate cancer growth with low adverse effects [25].

Sirtuin-2 inhibitors

Sirtuin-2 (SIRT2) is a member of the NAD^+-dependent histone deacetylase family, which has recently received increased attention because of its potential involvement in cancer progression and neurodegenerative diseases. Based on the crystallographic overlay of SIRT2–**43** with the complex of SirReal1–AcLys OTC

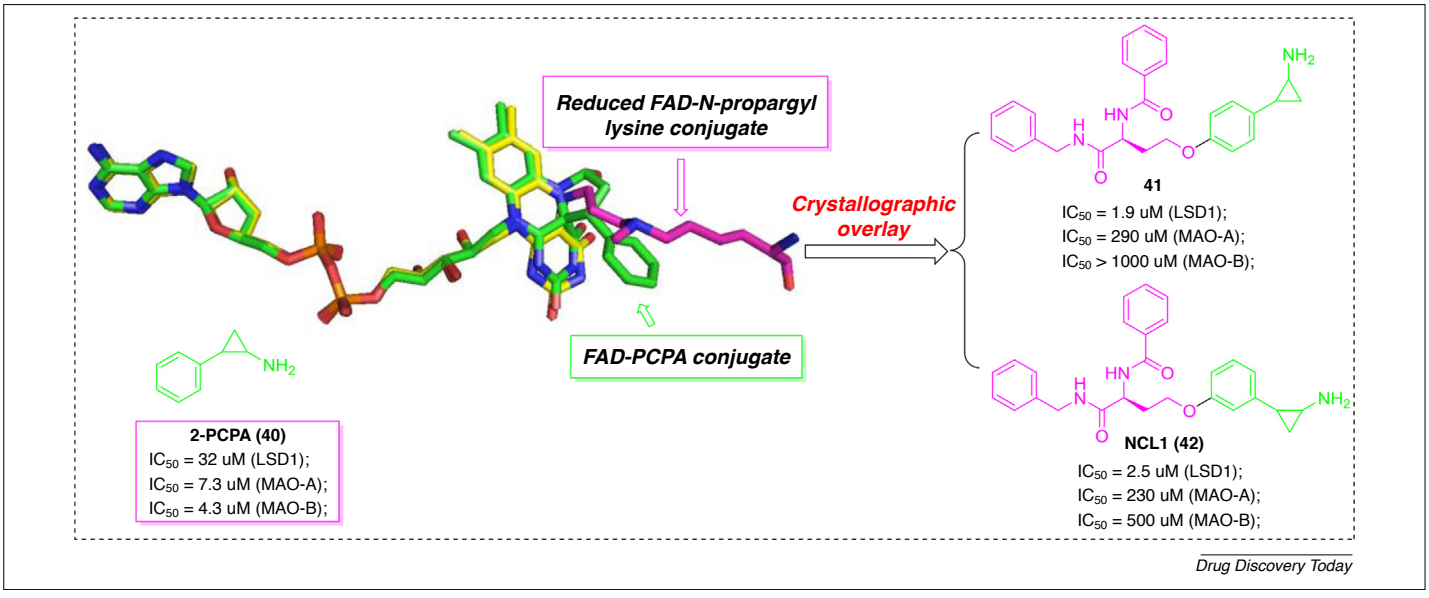

FIGURE 9

Development of cell-active LSD1-selective inhibitors via knowledge-based pharmacophore hybridization of the FAD-PCPA (**40**) conjugate (PDB code: 2UXX) and the reduced FAD-*N*-propargyl lysine peptide conjugate (PDB code: 2UXN) bound to the catalytic site of LSD1.

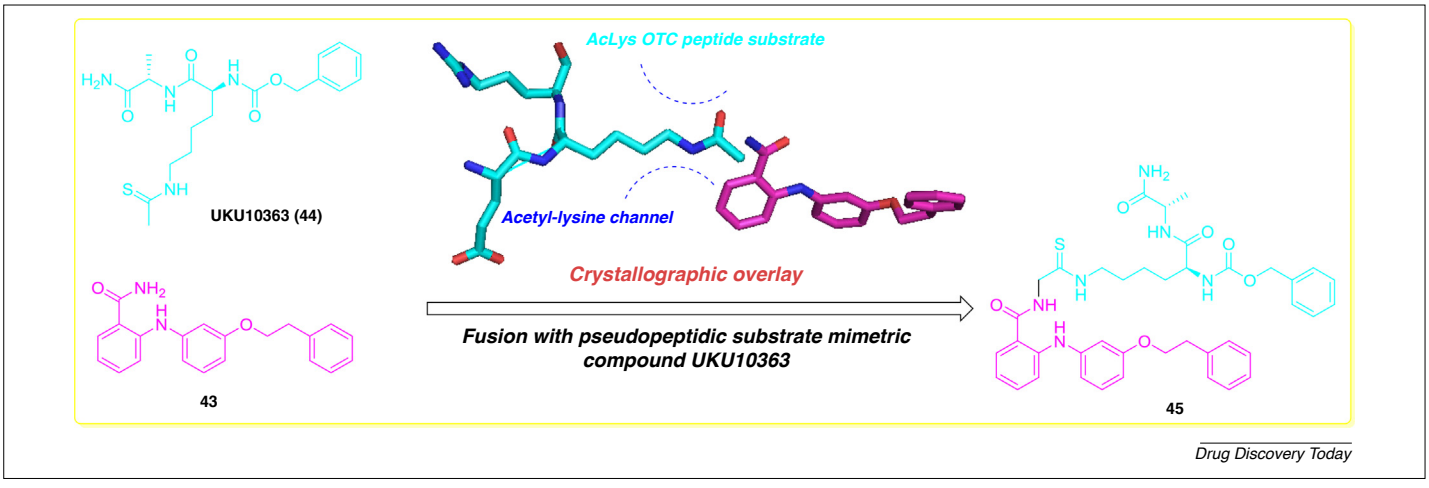

FIGURE 10

Application of molecular design to **43** to mimic acetyl–lysine substrate interactions. The structures of SIRT2–**43** complex (PDB code: 5Y5N) and the SirReal1–AcLys OTC peptide substrate complex (PDB: 4RMI) were superimposed.

peptide substrate [compound UKU10363 (**44**) is a pseudopeptidic substrate mimetic], the potent mechanism-based inactivator KPM-2 (**45**) was developed as a SIRT2-selective inhibitor with antiproliferative activity in cancer cells and remarkable neurite outgrowth-promoting potency (Fig. 10) [26].

To sum up, a detailed understanding of the interactions between the target protein and its binders provides an excellent basis for improving the affinity and selectivity of inhibitors via mechanism-based drug design [27]. This methodology is well illustrated by the discovery of LSD1- and SIRT2-selective inhibitors.

Concluding remarks and future perspectives

Drug discovery is a complex, costly and time-consuming campaign that involves multiple projects, ranging from target validation to clinical trials and regulatory approval. In particular, the search for drugs with novel mechanisms of action has become extremely expensive and risky. By contrast, follow-on programs to optimize or extend the scope of lead compounds with definite mechanisms are less costly and more likely to be successful but can generate drugs with meaningful differentiations from the leads. Crystallographic overlay-based molecular hybridization is essentially the common medicinal chemistry method of joining fragments of two known leads to create a new molecule. X-ray crystal structures of ligand-bound targets are overlaid, all overlapping regions in all pairs of ligands are observed and the fragments on each side of each matching region are swapped to create new compounds. This method can be applied recursively to produce all possible combinations of known leads. Because all of the binder functional moieties are known to bind to the target in the precise orientation and position present in the novel hybrid, this method is fast, and the success rate should be superior to those of traditional *de novo* design techniques. In an era of increasingly high-throughput X-ray co-crystallography of proteins with ligands, the optimization trajectory can be significantly expedited through application of a structure-based molecular hybridization approach.

The physicochemical properties of larger hybrid molecules are generally less drug-like than those of smaller molecules. If the degree of framework overlap is maximized and the size of the combined ligands is minimized, the likelihood of obtaining drug-like ligands with reasonable ligand efficiencies and favorable physicochemical properties can be maximized.

Usually, crystallographic overlay-based molecular hybridization is a fragment-growing optimization process. The tolerated solvent-exposed regions in the specific drug target provide a broad space for substantial modifications of existing molecules, with the aim of enhancing binding affinity, improving ligand efficiency, selectivity and physicochemical or pharmacokinetic properties. The possibility of discovering novel chemical entities that lie in unexplored regions of the crowded intellectual property landscape makes such follow-on campaigns attractive prospects.

Conflicts of interest

The authors declare that they have no conflicts of interest.

Acknowledgments

We gratefully acknowledge financial support from the National Natural Science Foundation of China (NSFC Nos. 81573347, 81603028), Young Scholars Program of Shandong University (YSPSDU No. 2016WLJH32), the Fundamental Research Funds of Shandong University (No. 2017JC006), Key Project of NSFC for International Cooperation (No. 81420108027), the Natural Science Foundation of Shandong Province (No. ZR2016HB26) and the Key Research and Development Project of Shandong Province (No. 2017CXGC1401). All figures showing binding modes were generated using PyMol (www.pymol.org).

References

1 Agarwal, D. *et al.* (2017) Are antimalarial hybrid molecules a close reality or a distant dream? *Antimicrob. Agents Chemother.* 61 e00249–17
2 Lazar, C. *et al.* (2004) Drug evolution concept in drug design: 1. Hybridization method. *J. Med. Chem.* 47, 6973–6982
3 Pierce, A.C. *et al.* (2004) BREED: generating novel inhibitors through hybridization of known ligands. Application to CDK2, p38, and HIV protease. *J. Med. Chem.* 47, 2768–2775
4 Song, Y. *et al.* (2014) Recent advances in the discovery and development of novel HIV-1 NNRTI platforms (Part II): 2009–2013 update. *Curr. Med. Chem* 21, 329–355
5 Zhan, P. *et al.* (2013) HIV-1 NNRTIs: structural diversity, pharmacophore similarity, and implications for drug design. *Med. Res. Rev.* 33 (Suppl. 1), E1–72
6 Zhan, P. *et al.* (2016) Anti-HIV drug discovery and development: current innovations and future trends. *J. Med. Chem.* 59, 2849–2878
7 Jones, L.H. *et al.* (2009) Novel indazole non-nucleoside reverse transcriptase inhibitors using molecular hybridization based on crystallographic overlays. *J. Med. Chem.* 52, 1219–1223
8 Huang, B. *et al.* (2017) Discovery of novel DAPY-IAS hybrid derivatives as potential HIV-1 inhibitors using molecular hybridization based on crystallographic overlays. *Bioorg. Med. Chem.* 25, 4397–4406
9 Zhang, H. *et al.* (2017) Discovery of uracil-bearing DAPYs derivatives as novel HIV-1 NNRTIs via crystallographic overlay-based molecular hybridization. *Eur. J. Med. Chem.* 130, 209–222
10 Liu, Z. *et al.* (2014) Design, synthesis and anti-HIV evaluation of novel diarylnicotinamide derivatives (DANAs) targeting the entrance channel of the NNRTI binding pocket through structure-guided molecular hybridization. *Eur. J. Med. Chem.* 87, 52–62
11 Chen, W. *et al.* (2014) Discovery of 2-pyridone derivatives as potent HIV-1 NNRTIs using molecular hybridization based on crystallographic overlays. *Bioorg. Med. Chem.* 22, 1863–1872
12 Kertesz, D.J. *et al.* (2010) Discovery of piperidin-4-yl-aminopyrimidines as HIV-1 reverse transcriptase inhibitors. *N*-benzyl derivatives with broad potency against resistant mutant viruses. *Bioorg. Med. Chem. Lett.* 20, 4215–4218
13 Bungard, C.J. *et al.* (2017) Design and synthesis of piperazine sulfonamide cores leading to highly potent HIV-1 protease inhibitors. *ACS Med. Chem. Lett.* 8, 1292–1297
14 Gràcia, J. *et al.* (2016) Biphenyl pyridazinone derivatives as inhaled pde4 inhibitors: structural biology and structure-activity relationships. *J. Med. Chem.* 59, 10479–10497
15 Roberts, R.S. *et al.* (2018) 4-Amino-7,8-dihydro-1,6-naphthyridin-5(6h)-ones as inhaled phosphodiesterase type 4 (PDE4) inhibitors: structural biology and structure-activity relationships. *J. Med. Chem.* 61, 2472–2489
16 Murray, C.W. *et al.* (2015) Fragment-based discovery of potent and selective DDR1/2 inhibitors. *ACS Med. Chem. Lett.* 6, 798–803
17 Zhan, P. *et al.* (2014) Recent advances in the structure-based rational design of TNKSIs. *Mol. Biosyst.* 10, 2783–2799
18 Bregman, H. *et al.* (2013) Discovery of novel, induced-pocket binding oxazolidinones as potent, selective, and orally bioavailable tankyrase inhibitors. *J. Med. Chem.* 56, 4320–4342
19 Huang, H. *et al.* (2013) Structure-based design of 2-aminopyridine oxazolidinones as potent and selective tankyrase inhibitors. *ACS Med. Chem. Lett.* 4, 1218–1223
20 Anumala, U.R. *et al.* (2017) Discovery of a novel series of tankyrase inhibitors by a hybridization approach. *J. Med. Chem.* 60, 10013–10025
21 Hutton, J.A. *et al.* (2014) Structure-based design of potent and selective *Leishmania N*-myristoyltransferase inhibitors. *J. Med. Chem.* 57, 8664–8670
22 Lorthiois, E. *et al.* (2017) Discovery of highly potent and selective small-molecule reversible factor D inhibitors demonstrating alternative complement pathway inhibition *in vivo*. *J. Med. Chem.* 60, 5717–5735

23 Keune, W.J. *et al.* (2017) Rational design of autotaxin inhibitors by structural evolution of endogenous modulators. *J. Med. Chem.* 60, 2006–2017
24 Wang, X. *et al.* (2015) Medicinal chemistry insights in the discovery of novel LSD1 inhibitors. *Epigenomics* 7, 1379–1396
25 Ueda, R. *et al.* (2009) Identification of cell-active lysine specific demethylase 1-selective inhibitors. *J. Am. Chem. Soc.* 131, 17536–17537
26 Mellini, P. *et al.* (2017) Potent mechanism-based sirtuin-2-selective inhibition by an in situ-generated occupant of the substrate-binding site, "selectivity pocket" and NAD^+-binding site. *Chem. Sci.* 8, 6400–6408
27 Zhan, P. *et al.* (2015) Strategies for the discovery of target-specific or isoform-selective modulators. *J. Med. Chem.* 58, 7611–7633